BJR https://doi.org/10.1259/bjr.20180074

Received: 14 January 2018 | Revised: 04 April 2018 | Accepted: 10 April 2018

Cite this article as:
Müller C, Domnanich KA, Umbricht CA, van der Meulen NP. Scandium and terbium radionuclides for radiotheranostics: current state of development towards clinical application. *Br J Radiol* 2018; **91**: 20180074.

THERANOSTICS AND PRECISION MEDICINE SPECIAL FEATURE: REVIEW ARTICLE

Scandium and terbium radionuclides for radiotheranostics: current state of development towards clinical application

[1]CRISTINA MÜLLER, PhD, [2]KATHARINA A DOMNANICH, [1]CHRISTOPH A UMBRICHT and [1,2]NICHOLAS P VAN DER MEULEN

[1]Center for Radiopharmaceutical Sciences ETH-PSI-USZ, Paul Scherrer Institut, Villigen-PSI, Switzerland
[2]Laboratory of Radiochemistry, Paul Scherrer Institut, Villigen-PSI, Switzerland

Address correspondence to: Dr Cristina Müller
E-mail: *cristina.mueller@psi.ch*

ABSTRACT

Currently, different radiometals are in use for imaging and therapy in nuclear medicine: ^{68}Ga and ^{111}In are examples of nuclides for positron emission tomography (PET) and single photon emission computed tomography (SPECT), respectively, while ^{177}Lu and ^{225}Ac are used for β^-- and α-radionuclide therapy. The application of diagnostic and therapeutic radionuclides of the same element (radioisotopes) would utilize chemically-identical radiopharmaceuticals for imaging and subsequent treatment, thereby enabling the radiotheranostic concept. There are two elements which are of particular interest in this regard: Scandium and Terbium. Scandium presents three radioisotopes for theranostic application. ^{43}Sc ($T_{1/2}$ = 3.9 h) and ^{44}Sc ($T_{1/2}$ = 4.0 h) can both be used for PET, while ^{47}Sc ($T_{1/2}$ = 3.35 d) is the therapeutic match—also suitable for SPECT. Currently, ^{44}Sc is most advanced in terms of production, as well as with pre-clinical investigations, and has already been employed in proof-of-concept studies in patients. Even though the production of ^{43}Sc may be more challenging, it would be advantageous due to the absence of high-energetic γ-ray emission. The development of ^{47}Sc is still in its infancy, however, its therapeutic potential has been demonstrated preclinically. Terbium is unique in that it represents four medically-interesting radioisotopes. ^{155}Tb ($T_{1/2}$ = 5.32 d) and ^{152}Tb ($T_{1/2}$ = 17.5 h) can be used for SPECT and PET, respectively. Both radioisotopes were produced and tested preclinically. ^{152}Tb has been the first Tb isotope that was tested (as ^{152}Tb-DOTATOC) in a patient. Both radionuclides may be of interest for dosimetry purposes prior to the application of radiolanthanide therapy. The decay properties of ^{161}Tb ($T_{1/2}$ = 6.89 d) are similar to ^{177}Lu, but the coemission of Auger electrons make it attractive for a combined β^-/Auger electron therapy, which was shown to be effective in preclinical experiments. ^{149}Tb ($T_{1/2}$ = 4.1 h) has been proposed for targeted α-therapy with the possibility of PET imaging. In terms of production, ^{161}Tb and ^{155}Tb are most promising to be made available at the large quantities suitable for future clinical translation. This review article is dedicated to the production routes, the methods of separating the radioisotopes from the target material, preclinical investigations and clinical proof-of-concept studies of Sc and Tb radionuclides. The availability, challenges of production and first (pre)clinical application, as well as the potential of these novel radionuclides for future application in nuclear medicine, are discussed.

INTRODUCTION

In nuclear medicine, the term "theranostics" refers to the application of radiopharmaceuticals for diagnosis and therapy.[1] Radionuclides emitting γ-radiation or positrons can be used for single photon emission computed tomography (SPECT) and positron emission tomography (PET), respectively. The visualization of accumulated radioactivity and its quantification for dosimetry can provide important information towards the application of radionuclide therapy using the same targeting agent. The basic principle of radiotheranostics when using radioisotopes of the same element was applied more than 70 years ago in thyroid cancer patients.[2] This idea was conceptualized by Dr S. Hertz and realized by treating the first patient with radioiodine in 1941.[3,4] For several decades, radioiodine has been employed in clinical routine,[5] however, the use of radiometals towards the same principle has been more challenging. Currently, somatostatin analogs are used in

Table 1. Relevant decay characteristics of Sc and Tb isotopes

Isotope	Half-life	β^+ $E_{average}$ [keV] (I)	x and γ with I > 10% E [keV] (I)	β^- $E_{average}$ [keV] (I)	Conv. & Auger electrons (>1 keV) $E_{average}$ [keV] (I)	α E [keV] (I)
^{43}Sc	3.9 h	476 (88%)	372 (23%)	–		–
^{44}Sc	4.0 h	632 (94%)	1157 (100%)	–		–
^{47}Sc	3.35 d	–	159 (68%)	162 (100%)		–
^{149}Tb	4.1 h	730 (7%)	42–50 (69%), 165 (26%), 352 (29%), etc.	–	32 (85%)	3967 (17%)
^{152}Tb	17.5 h	1140 (20%)	42–50 (65%), 344 (64%)	–	36 (69%)	–
^{155}Tb	5.32 d	–	42–50 (108%), 87 (32%), 105 (25%)	–	19 (204%)	–
^{161}Tb	6.89 d	–	45–53 (39%), 75 (10%)	154 (100%)	19 (227%)	–

combination with ^{68}Ga for PET imaging and, in some cases, with ^{111}In for SPECT prior to β^--radionuclide therapy using ^{177}Lu $T_{1/2}$ = 6.65 d; $E\beta^-_{average}$ = 134 keV; Eγ=113 keV, 208 keV or ^{90}Y $T_{1/2}$ = 2.67 d; $E\beta^-_{average}$ = 933 keV.[6,7] The same concept was applied with prostate-specific membrane antigen (PSMA)-targeting ligands that have recently been introduced in clinical practice for PET imaging and therapy.[8–10] In some cases, α-emitters, such as ^{225}Ac and ^{213}Bi, were also combined with PSMA ligands for the treatment of patients with advanced prostate cancer.[11,12] In these, and many other, examples, the diagnostic radiometal was always a different element to the therapeutic counterpart. Radionuclides of the same element (*i.e.* radioisotopes) would allow the preparation of chemically-identical radiopharmaceuticals for diagnosis and therapy enabling the concept of radiotheranostics in the truest sense. In this regard, scandium and terbium are of particular interest, as they present several radioisotopes which may be of particular value for clinical translation.

Scandium has attracted the attention of researchers and nuclear physicians alike, due to the existence of matched radionuclides for the possibility of theranostic applications (Table 1).[13–15] ^{43}Sc and ^{44}Sc are promising for PET imaging. ^{47}Sc is a β^--emitter suitable for therapeutic purposes, which also produces γ-ray emission useful for SPECT imaging. The application of ^{43}Sc/^{44}Sc ($T_{1/2}$ = 3.9 and 4.0 h, respectively) for PET would be advantageous with regard to several aspects when comparing it to the currently-employed ^{68}Ga ($T_{1/2}$ = 68 min): the almost fourfold longer half-lives of ^{43}Sc/^{44}Sc would enable the shipment of ^{43}Sc/^{44}Sc-radiopharmaceuticals to distant PET centers. In addition, images could be acquired over longer periods. Finally, the stable co-ordination of Sc with 1,4,7,10-tetraazacyclododecane-1,4,7,10-tetraacetic acid (DOTA) allows the application of the same targeting agents as will subsequently be used for therapeutic applications.[16] ^{43}Sc/^{44}Sc may, therefore, be employed for diagnosis, as well as for planning and monitoring targeted radionuclide therapy with ^{177}Lu and ^{90}Y. The exact matched therapeutic counterpart, ^{47}Sc, would be even more appealing, as it can enable the concept of using chemically-identical radiopharmaceuticals with the same kinetic properties for diagnosis and therapy.

Terbium is unique in that it represents radioisotopes for all four modalities in nuclear medicine (Table 1).[17] ^{155}Tb emits γ-radiation for SPECT imaging and ^{152}Tb decays by the emission of positrons useful for PET. The decay of ^{161}Tb is characterized by the emission of low-energy β^--particles and γ-rays, similar to ^{177}Lu but, additionally, comprises a significant number of Auger/conversion electrons (~12 e^-/decay). It is, therefore, a promising candidate for therapeutic purposes.[18–20] ^{149}Tb decays by the emission of α-particles, potentially allowing its use for α-therapy.[21] Since terbium belongs to the group of lanthanides, stable coordination is feasible with DOTA, a macrocyclic chelator that is commonly used for chelation of ^{177}Lu. The production of Tb nuclides and its chemical (lanthanide) separation are not trivial processes, which may explain why Tb radioisotopes have not been translated to clinical routine yet.

Scandium and terbium are not only related in that they present several medically-interesting radioisotopes, but they also have similar chemical properties, allowing the coordination of the same chelator and, hence, the same targeting agent.

Herein, we report on the production routes and separation methods of Sc and Tb radionuclides and summarize the application of the respective radioisotopes in preclinical settings. The first clinical proof-of-concept studies using Sc and Tb radionuclides are also presented. The availability, challenges of production and the potential of these novel radionuclides for future application in nuclear medicine are discussed.

PRODUCTION OF SCANDIUM AND TERBIUM RADIONUCLIDES

Production of scandium radioisotopes

^{44}Sc

The production of ^{44}Sc was initially proposed by the development of a ^{44}Ti/^{44}Sc generator.[22] The first such generator allowed elution of ~185 MBq ^{44}Sc in a volume of 20 ml.[23] A 10-min post-processing step of the ^{44}Sc eluate was established to reduce the volume and hydrochloric acid concentration, as well as to remove oxalate anions.[22,24] ^{44}Sc obtained via this production route was applied for the labeling of DOTATOC, allowing its application in a patient for the first time.[25] Recently, generator-produced ^{44}Sc was also used for the preparation of ^{44}Sc-PSMA-617 and injected into prostate cancer patients.[26]

Alternatively, the production of ^{44}Sc was proposed using natural calcium at a cyclotron.[27] Activities of up to 650 MBq ^{44}Sc were

Figure 1. Transversal sections of PET scans of Derenzo phantoms (hole diameter ranging from 0.8 to 1.3 mm in 0.1 mm increments; 1.0 and 1.3 indicate the holes of 1.0 mm and 1.3 mm diameter, respectively) filled with (a) > 99% ^{44}Sc, (b) 66.2% ^{43}Sc/33.3% ^{44}Sc and (c) 98.2% ^{43}Sc. The acquisition of the PET scans was performed within the energy window of 400–700 keV for 30 min, in order to obtain a total number of ~6 × 10^7 coincidences. Figure adapted from Domnanich et al. EJNMMI Radiopharmacy and Chemistry 2017; 2:14.[15] PET, positron emission tomography.

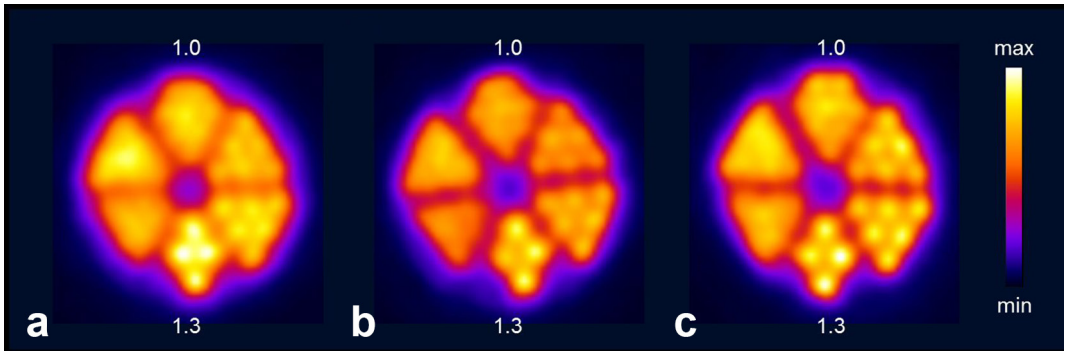

obtained after irradiation of the Ca target for 1 h, however, ^{44m}Sc, ^{47}Sc and ^{48}Sc were present in the final product as radioisotopic impurities. This may not be of concern for preclinical research, however, due to the long half-lives of these radioisotopes, it would be unfavorable for clinical application.[27,28] Krajewski et al reported the production of ^{44}Sc by irradiation of enriched ^{44}Ca targets at a cyclotron and investigated optimal proton beam energies to obtain the best ratio between ^{44}Sc and undesired ^{44m}Sc.[29] At the Paul Scherrer Institut (PSI), Switzerland, the production of ^{44}Sc from enriched ^{44}Ca at a cyclotron was investigated in detail, resulting in the first preclinical application of a ^{44}Sc-labeled biomolecule in tumor-bearing mice.[30] The irradiation process as well as the separation method based on extraction chromatography was optimized to enable the production of quantities of up to ~2 GBq radionuclidically pure ^{44}Sc when using proton beam energies of ~11 MeV.[14] These developments resulted in the first application of cyclotron-produced ^{44}Sc, in a clinical proof-of-concept study performed at Bad Berka, Germany.[31]

^{43}Sc

The cyclotron production of ^{43}Sc was proposed by proton irradiation of natural Ca targets for 1–2 h with α-particles, in an optimum energy range of 23.9–28.1 MeV to obtain activities for medical application.[32–35] The ^{43}Sc formation was induced via the nuclear reactions ^{40}Ca(α,p)^{43}Sc and ^{40}Ca(α,n)^{43}Ti→^{43}Sc. The formed products were of high radionuclidic purity (>99%) and impurities were below 1.5*10^{-5}% of the ^{43}Sc activity when irradiating enriched ^{40}Ca targets. Another option for the production of ^{43}Sc would be the irradiation of enriched ^{42}Ca targets with deuterons using the ^{42}Ca(d,n)^{43}Sc nuclear reaction, however, no experimental data were acquired to date. A drawback of these production routes is the limited availability of cyclotrons with high-current α-beams, as well as cyclotrons providing deuteron beams.[32,34]

Recently, the production of ^{43}Sc was investigated by comparing two different production routes based on proton irradiation of enriched ^{46}Ti and ^{43}Ca target material, respectively.[15] The production via the ^{46}Ti(p,α)^{43}Sc nuclear reaction yielded a modest ~200 MBq ^{43}Sc of high radionuclidic purity (>98%) at the end of a 7 h irradiation period when using 97% enriched ^{46}Ti.[15] The production via the ^{43}Ca(p,n)^{43}Sc nuclear reaction resulted in higher quantities of ^{43}Sc, but the product consisted of a mixture of ^{43}Sc and ^{44}Sc at an activity ratio of 2:1, when using 57.9% enriched $^{43}CaCO_3$.[15] PET images of Derenzo phantoms were acquired with ^{44}Sc obtained from irradiated ^{44}Ca targets, as well as with ^{43}Sc obtained via the ^{46}Ti-based production route or as a mixture with ^{44}Sc from ^{43}Ca irradiations. In line with the smaller positron energy of ^{43}Sc, the resolution was found to be the best for pure ^{43}Sc [full width at half maximum (FWHM) = 1.87 ± 0.14 mm], followed by the ^{43}Sc/^{44}Sc mixture (FWHM = 2.04 ± 0.06) and ^{44}Sc (FWHM = 2.12 ± 0.04) (Figure 1).[36]

^{47}Sc

The production of ^{47}Sc can be achieved via a number of different nuclear reactions using a cyclotron, reactor or electron linear accelerator. Misiak et al reported on the cyclotron production of ^{47}Sc via the ^{48}Ca(p,2n)^{47}Sc nuclear reaction.[37] Using a proton energy range of 24→17 MeV would be optimal for this purpose, however, the radionuclidic purity using this route was determined to be only ~87%. Using enriched ^{48}Ca for irradiation with 20 MeV protons may be a feasible route for the production of GBq activity levels of ^{47}Sc, however, the high cost of enriched ^{48}Ca has been prohibitive to investigate this production route to date.[37] An alternative route investigated the α-particle irradiation of ^{44}Ca targets at a cyclotron, inducing the ^{44}Ca(α,p)^{47}Sc nuclear reaction, but it provided a comparatively lower yield and radionuclidic purity.[35]

Domnanich et al investigated the production of ^{47}Sc by irradiation of ^{46}Ca targets in a high neutron flux reactor using the ^{46}Ca(n,γ)^{47}Ca→^{47}Sc nuclear reaction.[38] The produced ^{47}Ca decays to ^{47}Sc with a half-life of 4.5 days, hence, presenting an elegant generator-like concept enabling multiple separations of in-grown ^{47}Sc in an analogous process as described for the cyclotron-produced ^{44}Sc.[13] The same authors also reported on the irradiation of ^{47}Ti at a reactor to obtain ^{47}Sc via the ^{47}Ti(n,p)^{47}Sc nuclear reaction. This production route yielded low activities of ^{47}Sc which was accompanied with a high percentage of co-produced ^{46}Sc, however. Both characteristics are not desirable for radiopharmaceutical applications.[13] Similar findings were reported elsewhere.[39,40]

The method of ^{47}Sc production using electron linear accelerators (linacs) has also been proposed in the literature.[41,42] Mamtimin et al studied the production of ^{47}Sc via the ^{48}Ti(γ,p)^{47}Sc nuclear reaction by Monte Carlo simulations,[42] while Yagi et al and Rotsch et al reported preliminary experimental results obtained with enriched ^{48}Ti.[43,44] Irradiation of natural Ti targets would result in many different Sc radioisotopes and, thus, low specific activity of ^{47}Sc. Employing enriched ^{48}Ti targets when irradiating with 22 MeV beam would maximize the ^{47}Sc production and, simultaneously, minimize the formation of other unwanted Sc radionuclides.[42] Another option, reported by Starovoitova et al and Rane et al, was to use an electron linac to produce ^{47}Sc via the ^{48}Ca(γ,n)^{47}Ca→^{47}Sc nuclear reaction.[41,45]

Production of terbium radioisotopes

^{149}Tb, ^{152}Tb, ^{155}Tb

Based on calculations of excitation functions for light and heavy ion-induced reactions, Beyer et al suggested the ^{152}Gd(p,4n)^{149}Tb nuclear reaction as a promising route for the ^{149}Tb production.[21] Irradiation of even highly-enriched ^{152}Gd targets (which are not currently available) would presumably result in a mixture of various Tb radioisotopes, however.[17] Alternatively, ^{149}Tb could be produced via the indirect ^{142}Nd(^{12}C,5n)^{149}Dy→^{149}Tb or directly via the ^{141}Pr(^{12}C,4n)^{149}Tb nuclear reaction, but with only limited production yields and radionuclidic purity.[21] In initial experiments at the heavy ion cyclotron in Dubna, Russia, ^{149}Tb was produced by irradiation of a $^{nat}Nd_2O_3$ target for 1.25 h utilizing the indirect route to obtain a moderate yield of 2.7 MBq ^{149}Tb.[21] The production of ^{152}Tb at a cyclotron via the ^{152}Gd(p,n)^{152}Tb nuclear reaction would be problematic as well, because of the lack of highly-enriched target material and the formation of radioisotopic impurities. Proton irradiation of enriched ^{155}Gd via the ^{155}Gd(p,n)^{155}Tb reaction should be feasible to produce clinically-relevant quantities of ^{155}Tb, however.[46]

^{149}Tb, ^{152}Tb and ^{155}Tb were successfully produced by the high-energy proton irradiation of a tantalum foil target to induce spallation.[17] The spallation products were released from the target and ionized. Mass separation of the isotopes, along with their isobars and pseudoisobars, was carried out using the online mass separator at ISOLDE/CERN, Switzerland, as previously reported,[17] thereby, allowing the collection of the desired radionuclides in zinc-coated gold foils.[47,48] After dissolution of the zinc layer of the foil, the ^{149}Tb, ^{152}Tb or ^{155}Tb were separated from the matrix and its isobar and pseudoisobar impurities, respectively, using cation exchange chromatography and α-hydroxyisobutyric acid as eluent. This procedure provided the final product in α-hydroxyisobutyric acid solution at pH 4.75 enabling direct radiolabeling of tumor-targeting ligands.[17]

^{161}Tb

The production of ^{161}Tb was proposed by Lehenberger et al using the ^{160}Gd(n,γ)^{161}Gd→^{161}Tb nuclear reaction, a similar concept to the production of no-carrier added ^{177}Lu (Figure 2).[19] Highly-enriched ^{160}Gd targets were irradiated for 2–3 weeks at the spallation-induced neutron source at PSI or for 1 week at the high neutron flux nuclear reactor at Institut Laue-Langevin, France.[17] The product was separated from the Gd target material using ion exchange chromatographic methods to ensure provision of the final product in a small volume of dilute hydrochloric acid, as is the case for the commercially available ^{177}Lu.[17,19]

PRECLINICAL APPLICATIONS

Scandium radioisotopes

In order to obtain stable conjugation of scandium radioisotopes with tumor-targeting agents, the topic of chelation had to be addressed. Various open-chain polyamino-polycarboxylate ligands and macrocycles were investigated for their suitability to coordinate Sc.[16,49] It was determined that open-chain chelators formed complexes with Sc much faster than DOTA.[49] On the other hand, DOTA bound Sc nuclides more efficiently, as compared to 1,4 7-triazacyclononane-1,47-triacetic acid (NOTA) and 1,4,7-triazacyclodecane-1,4,7-triacetic acid (10-ane).[16] DOTA chelators with one methylphosphonic/phosphinic acid pendent arm (DO3AP, DO3AP^{PrA} and D3AP^{ABn}) were investigated as alternative chelators.[50] Another possibility for the coordination of Sc could be to use the 1,4-bis(carboxymethyl)−6-[bis(carboxymethyl)]amino-6-methylperhydro-1,4-diazepine (AAZTA) chelator, allowing radiolabeling under mild conditions (room temperature).[51] Chakravatry et al labeled

Figure 2. (a) Production route of no-carrier-added ^{177}Lu via the ^{176}Yb(n,γ)^{177}Yb→^{177}Lu nuclear reaction. (b) Analogous production route of ^{161}Tb via the ^{160}Gd(n,γ)^{161}Gd→^{161}Tb nuclear reaction. Figure adapted from Karlsruhe nuclide chart, 8th edition, 2012 (https://www.nucleonica.com/).

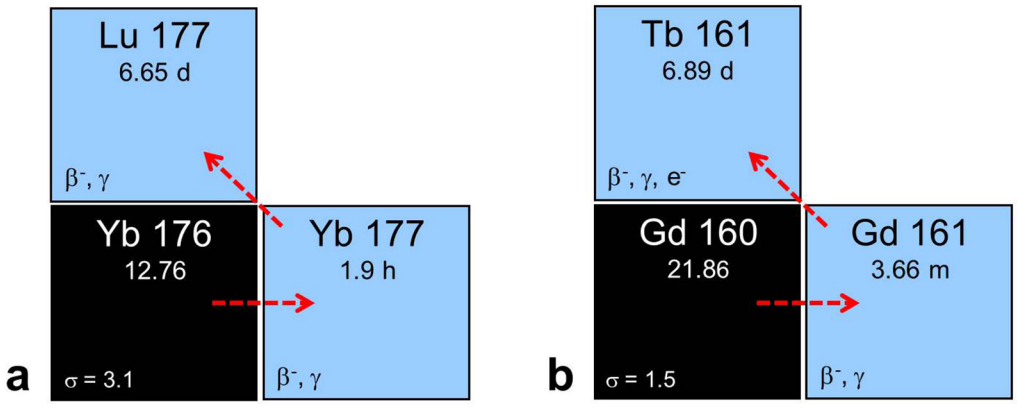

a CHX-A″-DTPA-functionalized antibody Fab fragment at room temperature within 45 min, resulting in >60% yield at an appreciable specific activity.[52] CHX-A″-DTPA is known to form more stable complexes than DTPA chelators and, hence, demonstrated stable coordination of ^{44}Sc in mouse serum over 6 h at 37°C.[52]

^{44}Sc

^{44}Sc was used for the radiolabeling of a variety of ligands, including somatostatin analogs,[53–55] a bombesin analog,[56] RGD peptides,[57] folate derivatives[30] and PSMA ligands.[58] Pre-clinical experiments, including PET imaging, were performed in mice bearing tumors that express the target of interest. Eigner et al reported on the use of generator-produced ^{44}Sc, in combination with a DOTA-derivatized puromycin.[59] It allowed the visualization of Walker carcinoma 256 (rat breast carcinoma) and AT1 carcinoma (subline of Dunning R3327 rat prostate carcinoma) tumors via PET imaging in rats due to protein synthesis-specific accumulation of ^{44}Sc-DOTA-puromycin.[59] Among the first pre-clinical experiments performed with cyclotron-produced ^{44}Sc was the study reported by Müller et al, where ^{44}Sc-folate was investigated *in vitro* using KB cells (human cervical cancer cells) as well as in KB tumor-bearing mice.[30] In this study, it was also shown that the tissue distribution profile of ^{44}Sc-folate was equal to that of ^{177}Lu-folate. The authors concluded that ^{44}Sc could serve for dosimetry purposes prior to ^{177}Lu-based radionuclide therapy in a clinical setting.[30] A similar pre-clinical setting was employed by the same authors using PSMA-617 for labeling with ^{44}Sc, ^{177}Lu and ^{68}Ga to compare the radionuclides' influence on the overall *in vitro* and *in vivo* behavior.[58] It was found that ^{44}Sc-PSMA-617 most closely resembled the ^{177}Lu-labeled version, showing almost identical *in vitro* properties and biodistribution data and, hence, representing the concept of radiotheranostics. Domnanich et al demonstrated that a DOTA chelator is more suitable for ^{44}Sc complexation compared to NODAGA by using two pairs of peptides, DOTA/NODAGA-RGD and DOTA/NODAGA-NOC, respectively.[55] In this regard, the behavior of ^{44}Sc was opposite to that of ^{68}Ga, which exhibited an increased stability when using NODAGA-functionalized peptides.[55] While labeling of small molecules and peptides with ^{44}Sc was exemplified many times, only few studies were reported about the ^{44}Sc-labeling of proteins. Among those was the application of ^{44}Sc for the labeling of a CHX-A"-DTPA-functionalized Fab fragment of Cetuximab, a chimeric human-murine IgG1 monoclonal antibody that binds specifically to the epidermal growth factor receptor.[52] Serial PET scans over a 6 h period revealed rapid and epidermal growth factor receptor-specific accumulation in U87MG tumors (human glioblastoma cell line) in a xenograft mouse model. Renal clearance was prominent, resulting in extensive accumulation of activity in the kidneys, whereas excretion via the hepatobiliary route was also observed.[52] Based on these promising results, the development of new ^{44}Sc-based radiopharmaceuticals for immunoPET imaging was encouraged by the authors.[52] Another study investigated ^{44}Sc in combination with an anti-HER2 affibody molecule (DOTA-$Z_{HER2:2891}$).[60] Affibody molecules are small scaffold proteins (58 amino acids, 7 kDa), known to refold after denaturation at elevated temperatures, hence, labeling at 95°C was possible.[61] The ^{44}Sc-DOTA-$Z_{HER2:2891}$ was investigated *in vitro* and *in vivo*, using HER2-positive SKOV-3.ip tumor cells (human ovarian cancer cells) and in mouse SKOV-3.ip xenograft models. HER2-specific tumor uptake was demonstrated in biodistribution studies and increased tumor-to-background contrast was achieved at delayed time points (6 h after injection), due to the longer half-life of ^{44}Sc as compared to ^{68}Ga.[60]

^{43}Sc

Radiolabeling of DOTA and DOTA-functionalized somatostatin receptor analogs (DOTATATE and DOTANOC) using ^{43}Sc has been successfully demonstrated,[15,32,35] however, pre-clinical studies using this radionuclide have not been published to date. In a recent study performed at PSI by the authors of this article, ^{43}Sc was used for the labeling of PSMA-617. ^{43}Sc-PSMA-617 was injected into a mouse bearing PC-3 PIP/flu tumors (PSMA-positive and PSMA-negative prostate cancer cells, respectively) for PET/CT imaging at different time points after injection (unpublished data), as was previously reported by Umbricht et al for ^{44}Sc-PSMA-617.[58] The same was also done with ^{44}Sc- and ^{47}Sc-labeled PSMA-617 for PET and SPECT imaging, respectively. The obtained images of mice that received ^{43}Sc-, ^{44}Sc- and ^{47}Sc-labeled PSMA-617 are shown in Figure 3. The *in vivo* behavior of these chemically-identical radioligands is the same, independent of the Sc radioisotope employed. The result may be slightly improved in the case of ^{43}Sc when compared to ^{44}Sc, however, this was only visible in pre-clinical phantom studies.[15] More importantly, there is the possibility of reducing the dose burden when using ^{43}Sc, due to the absence of high-energy γ-radiation as emitted by ^{44}Sc.

^{47}Sc

The concept of theranostic application (PET/β^--therapy) with the matched pair of ^{44}Sc/^{47}Sc radionuclides was proposed and exemplified in a preclinical study using a DOTA-folate conjugate.[13] ^{44}Sc-folate resulted in distinct visualization of FR-positive KB tumors using PET. The therapeutic potential of ^{47}Sc-folate was successfully demonstrated by a delay in tumor growth and an increased survival time of treated mice, compared to an untreated control group.[13]

Terbium radioisotopes

Preclinical application of all four terbium radioisotopes has been reported by Müller et al in 2012, when a proof-of-concept study was performed with a DOTA-folate conjugate in a folate receptor-positive tumor mouse model.[17] This study demonstrated the feasibility of using ^{152}Tb and ^{155}Tb for PET and SPECT imaging, respectively, as well as the potential of using ^{149}Tb and ^{161}Tb for α- and β^--/Auger -electron therapy, respectively.

^{152}Tb

Due to an increased production yield achieved in recent years at ISOLDE/CERN, Switzerland, it was possible to investigate ^{152}Tb in a more detailed study using a mouse model of somatostatin receptor-positive AR42J rat tumor xenografts (rat pancreatic cancer cells).[62] DOTANOC, a clinically-established somatostatin analog, was labeled at variable specific activity and used for imaging purposes using a pre-clinical PET/CT scanner.[62]

Figure 3. PET/CT and SPECT/CT images as MIPs of mice 2 h after injection of (a) ^{43}Sc-PSMA-617, (b) ^{44}Sc-PSMA-617 and (c) ^{47}Sc-PSMA-617. PSMA-=PC-3 flu tumor; PSMA+=PC-3 PIP tumor, Ki = kidney, Bl = urinary bladder. The PET/CT and SPECT/CT images were prepared using VivoQuant software. The scales of PET and SPECT images were cut by 1 and 10%, respectively, to make the accumulated activity in tumors and kidneys better visible (unpublished results). Bl, urinary bladder; Ki, kidney; MIPs, maximum intensity projections; PET, positron emission tomography; PSMA, prostate-specific membrane antigen; SPECT, single photon emission computed tomography.

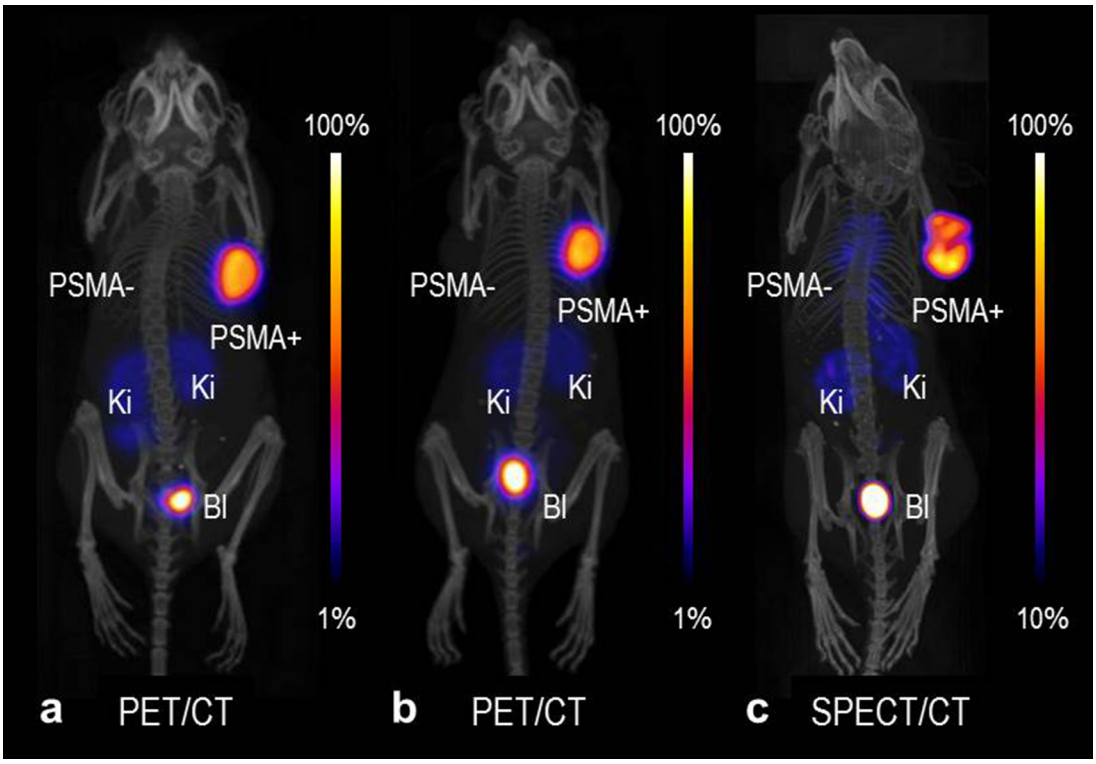

The tissue distribution profile of ^{152}Tb-DOTANOC was equal to that of ^{177}Lu-DOTANOC when applied to in the same animal model, showing favorable tumor-to-background ratios at higher specific activities.[62] These results confirmed the assumption that the ^{152}Tb-labeled compound would show the same *in vivo* behavior as its ^{177}Lu-labeled match and could, therefore, be used for imaging and dosimetry prior to ^{177}Lu-based radionuclide therapy. In this regard, and in view of the application in combination with longer-circulating radioligands and antibodies, the 17.5 h half-life of ^{152}Tb would be considered an advantage.[62]

^{155}Tb

The γ-ray energies of ^{155}Tb make this radionuclide well suited for SPECT imaging (Table 1). Derenzo phantom studies performed with ^{155}Tb showed an excellent spatial resolution compared to that obtained with the clinically-established SPECT nuclide ^{111}In ($T_{1/2}$ = 2.80 d, Eγ=171 keV and 245 keV; Figure 4).[63] SPECT/CT imaging was investigated using fast-clearing DOTA-peptides, including a minigastrin-based peptide and DOTATATE, as well as longer-circulating biomolecules such as an albumin-binding DOTA-folate (cm09) and the L1-cell adhesion molecule (L1-CAM)-antibody chCE7. These biomolecules were labeled with ^{155}Tb and used for preclinical imaging of tumor-bearing mice 4 h after injection of the radiolabeled peptides or 2 days and 3 days after injection of ^{155}Tb-folate and ^{155}Tb-chCE7, respectively.[63] The images were of high quality, enabling visualization of even small lesions in the abdominal region, as well as in the liver of an intraperitoneal SKOV-3.ip tumor mouse model, days after injection of ^{155}Tb-chCE7. ^{155}Tb was proposed as an alternative option to ^{111}In for dosimetry planning prior to the application of lanthanide-based radionuclide therapy.[63]

^{149}Tb

The first pre-clinical application of ^{149}Tb was reported by Beyer et al.[64] A SCID mouse model of leukemia was used to demonstrate

Figure 4. SPECT images of Derenzo phantoms filled with (a) ^{155}Tb (2.6 MBq) and (b) ^{111}In (4 MBq). Figure adapted from Müller et al. Nucl Med Biol 2014;41 Suppl:e58-65.3][63] SPECT, single photon emission computed tomography.

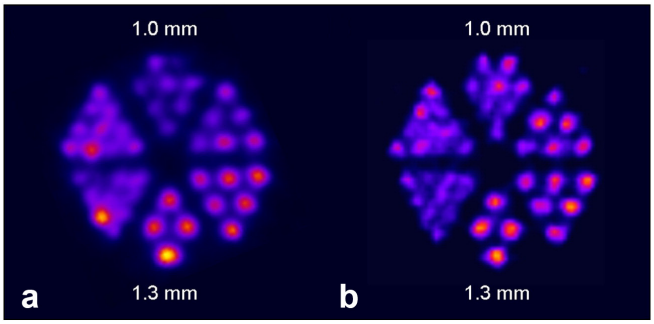

Figure 5. MIP of PET/CT image of AR42J tumor-bearing mouse 2 h after injection of ^{149}Tb-DOTATOC (7 MBq). Figure adapted from Müller et al. EJNMMI Radiopharmacy and Chemistry 2016;1:5.[66] Bl, urinary bladder; Ki, kidney; MIP, maximum intensity projection; PET, positron emission tomography; Tu, tumor.

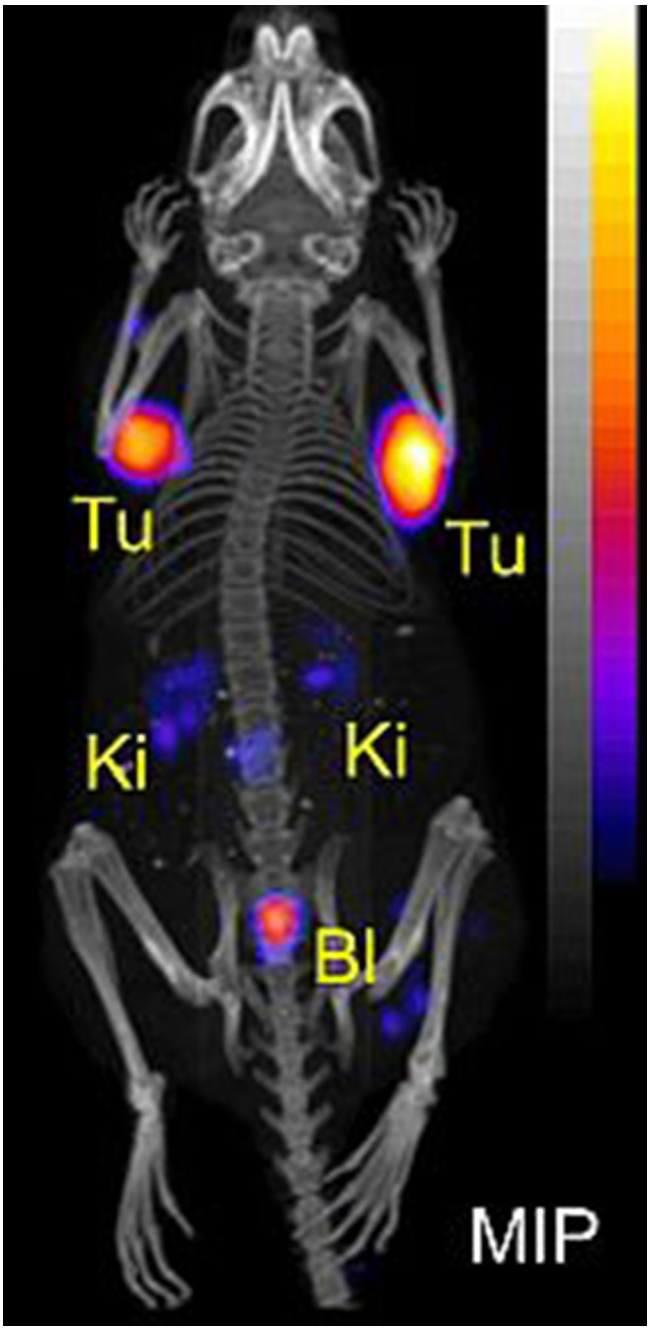

the effect of ^{149}Tb-labeled rituximab, a CD20-targeted antibody outfitted with CHX-A-DTPA chelators.[64] Mice were administered with the radioimmunoconjugate (5.5 MBq, 5 μg per mouse) 2 days after intravenous injection of 5 million Daudi cells (human Burkitt lymphoma cells) before the appearance of manifested tumors. In 89% of the treated mice, the therapy resulted in tumor-free survival of more than 4 months, a significant increase in survival time as compared to the other groups.[64] Untreated animals developed signs of Burkitt lymphoma, which required euthanasia within 37 days.[64] Animals treated with a low dose of unlabeled rituximab (5 μg per mouse) had to be euthanized within 43 days, while the treatment with a high dose of rituximab (300 μg per mouse) increased the lifetime, resulting in a median survival of 100 days. Preliminary dose estimation for humans reported by Beyer et al revealed that a therapeutic activity of 5 GBq ^{149}Tb-rituximab would result in a bone marrow radiation dose far below the critical level.[64] ^{149}Tb was also used for targeted radionuclide therapy using a DOTA-folate conjugate in a proof-of-concept study with KB tumor-bearing mice.[17] At a later stage, the same model was used to investigate two different activity levels (2.2 MBq and 3.0 MBq per mouse, respectively) of ^{149}Tb-folate. A dose-dependent effect was observed with regard to the tumor growth delay, as well as the median survival time which was increased to 30.5 day and 43 days, respectively, as compared to a median survival of 21 days in the case of untreated control animals.[65] The therapeutic effect of ^{149}Tb-folate was also confirmed *in vitro*, where the radiofolate reduced the tumor cell survival in a FR-specific manner.[65] More recently, it was demonstrated for the first time in a pre-clinical setting that, based on the coemission of positrons, ^{149}Tb can be used for PET imaging.[66] An AR42J tumor-bearing mouse was injected with ^{149}Tb-DOTANOC (7 MBq) followed by PET/CT imaging 2 h later. The high-quality images allowed distinct visualization of the tumor xenografts (Figure 5). The concept of α-PET is entirely novel and would make ^{149}Tb attractive for future clinical translation, potentially allowing the visualization of applied ^{149}Tb-radioligands.

^{161}Tb

De Jong et al reported on the first preclinical study performed with ^{161}Tb in 1995 using ^{161}Tb-octreotide to investigate the biodistribution in normal rats.[67] It was found that ^{161}Tb-octreotide cleared faster from the blood than ^{111}In-octreotide, however, liver uptake was higher for the ^{161}Tb-labeled version.[67] The uptake in somatostatin receptor-positive tissues, such as CA20948 tumor (rat pancreatic cell line), pancreas and adrenals, was shown to be specific. Based on the results of this study, the authors concluded that ^{161}Tb would be of interest for intraoperative imaging and radionuclide therapy.[67] The first therapy study was reported in 2012, with a small number of KB tumor-bearing mice using a ^{161}Tb-folate for a proof-of-concept investigation, where its potential for tumor growth inhibition was demonstrated (Figure 6).[17]

The imaging potential using pre-clinical SPECT, as well as the therapeutic effect of ^{161}Tb-folate, was investigated in a one-to-one comparison with ^{177}Lu-folate and FR-positive KB and IGROV-1 tumor xenografts, respectively.[68] In line with the increased mean absorbed tumor dose after administration of ^{161}Tb-folate, it was more effective to treat KB tumors than ^{177}Lu-folate applied at the same activity. As a consequence, the median survival time in ^{161}Tb-folate treated mice was increased (54 days) as compared to mice treated with ^{177}Lu-folate (35 day) or control mice (31 days) in the KB tumor models. The same held true for IGROV-1 tumor mice, even though the difference in tumor growth delay and survival time was less pronounced. Both radiofolates produced high-resolution pre-clinical images of the tissue

Figure 6. Pre-clinical therapy study: the graph represents the tumor growth relative to the average tumor size (tumor volume) determined at Day 0, which was set to 1 (indicated as relative tumor size). The study was performed with five untreated mice (controls: green/blue) and five mice treated with ^{161}Tb-folate (11 MBq/mouse; red/orange). In the treated group, four of the five mice showed complete tumor remission as shown by overlapping graphs. This research was originally published in *JNM*, Müller et al.[17] PET, positron emission tomography; SPECT, single photon emission computed tomography.

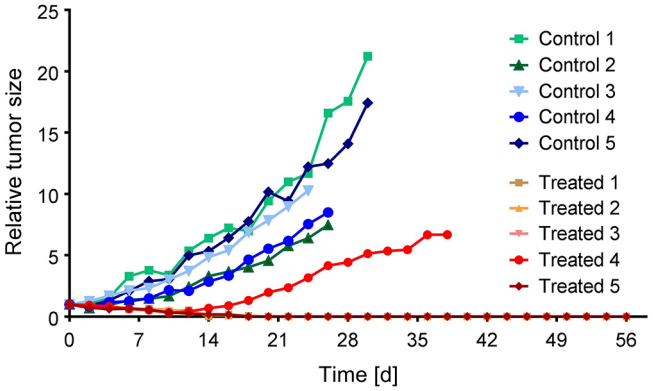

distribution profile in tumor-bearing mice. More recently, Haller et al conducted a study over 8 months in order to investigate and compare potential undesired side effects to the kidneys after ^{161}Tb- and ^{177}Lu-folate therapy, respectively.[69] The evaluation of kidney function, as well as histopathological analysis of the renal tissue, revealed a dose-dependent damage with increasing scores of 1, 3 and 4 after administration of ^{161}Tb-folate at 10, 20 and 30 MBq, respectively. These results were comparable to the damage (scored as 2, 3 and 4, respectively) after application of ^{177}Lu-folate at the same activities. The authors concluded that Auger electrons—even though they contributed to the mean absorbed kidney dose—did not cause additional renal damage.[69] The anti-L1-CAM antibody, chCE7, was also labeled with ^{161}Tb for direct comparison with the ^{177}Lu-labeled version.[70] ^{161}Tb-chCE7 showed higher radiotoxicity in nude mice (maximal tolerated dose: 10 MBq per mouse) as compared to ^{177}Lu-chCE7 (maximal tolerated dose: 12 MBq per mouse). At equitoxic doses, ^{161}Tb-chCE7 was, however, more effective tin the growth delay of IGROV-1 tumors when compared to ^{177}Lu-chCE7.[70]

CLINICAL PROOF-OF-CONCEPT STUDIES

Scandium-44

The first clinical application of generator-produced ^{44}Sc was performed in 2009.[22] PET scans were acquired of a patient injected with ^{44}Sc-DOTATOC, resulting in high-quality images up to 18 h after injection.[22] More recently, ^{44}Ti generator-produced ^{44}Sc was employed for a first-in-man study of using ^{44}Sc-PSMA-617.[26] Four male patients with histologically-proven prostate carcinoma, who were scheduled for ^{177}Lu-PSMA-617 therapy, were selected for the study. After the intravenous administration of ^{44}Sc-PSMA-617 (50.5 ± 9.3 MBq), the patients underwent a dynamic PET scan of the abdomen over a period of 30 min, followed by static PET/CT scans from skull to midthigh up to 18 h after injection (Figure 7).[26]

Accumulation of radioactivity was found in multiple soft tissue and skeletal metastases, whereas physiological radioligand uptake was observed in the kidneys, liver, spleen, small intestine, urinary bladder and salivary glands. The kidneys received the highest absorbed radiation dose (0.354 mSv/MBq) after application of ^{44}Sc-PSMA-617.[26] The PET images obtained at 2 h after administration of ^{44}Sc-PSMA-617 were compared to those obtained earlier using ^{68}Ga-PSMA-11. Visual assessment of the PET scan acquired with ^{44}Sc-PSMA-617 was at least of equal quality as the one obtained previously with ^{68}Ga-PSMA-11 (Figure 7). Quantitative analysis revealed no differences between uptake of ^{44}Sc-PSMA-617 and ^{68}Ga-PSMA-11 in most organs, however, reduced accumulation of ^{44}Sc-PSMA-617 was observed in the kidneys when compared to ^{68}Ga-PSMA-11.[26]

Singh et al were the first to report on a proof-of-concept imaging study in patients using ^{44}Sc produced at a cyclotron.[31] Due to the high yield (~2 GBq) obtained from this production method, it was possible to ship ^{44}Sc over a distance of 600 km from the production site at PSI, Switzerland, to Zentralklinik Bad Berka, Germany, requiring two half-lives' travel time. At Bad Berka, ^{44}Sc was used for the labeling of DOTATOC.[31] Two male patients with well-differentiated, non-functional and functional neuroendocrine neoplasm, respectively, were selected for this study. After injection of 78 MBq and 96 MBq ^{44}Sc-DOTATOC, eight sets of PET/CT scans were acquired at variable time points over a period of 24 h.[31] Distinct uptake of radioactivity was observed in malignant lesions already at early time points, with best tumor-to-background at about 4 h after injection.

The tissue distribution was somewhat different when compared with that of ^{68}Ga-DOTATOC (Figure 8), which may be attributed to the low specific activity of ^{44}Sc-DOTATOC (~1.4 MBq/μg, >55 μg). The authors stated that decreasing the amount of injected peptide to <50 μg would be the aim for future studies in this regard. ^{44}Sc-DOTATOC showed significant potential for PET/CT imaging and as a suitable diagnostic match to currently-used therapeutic radionuclides such as ^{177}Lu and ^{90}Y - as well as ^{47}Sc, once it becomes commercially available.[31]

Terbium-152

The production of ^{152}Tb at ISOLDE/CERN, followed by the chemical separation from catcher foils and impurities at PSI, resulted in a pure product in sufficient yields for use in a first-in-man application in 2016.[71] ^{152}Tb was used for labeling of DOTATOC at Zentralklinik, Bad Berka, and administered to a male patient with diagnosed metastatic, well-differentiated, functional neuroendocrine neoplasm of the terminal ileum.[71] PET/CT scans were performed for restaging of the disease 8 years after the sixth cycle of peptide receptor radionuclide therapy. The scans were acquired over a period of 24 h after injection of 145 MBq ^{152}Tb-DOTATOC.[71] The resulting images allowed visualization of even small metastases, with increased tumor-to-background contrast at later time points (Figure 9). It was concluded that ^{152}Tb would be of particular value for dosimetry prior to radionuclide therapy, due to its much longer half-life (17.5 h) enabling delayed PET scans, as compared to the very short half-life (68 min) of ^{68}Ga which cannot serve this purpose.[71]

Figure 7. MIP (top) and representative sections (bottom) of PET/CT examination of a patient suffering from mCRPC, with high tumor load, using (a) ^{44}Sc-PSMA-617 (50 MBq, 60 min p.i.), and (b) ^{68}Ga-PSMA-11 (120 MBq, 60 min p.i.). (c) On the right hand side, the planar scintigraphy is shown (top) and a representative section of the post-therapy SPECT/CT scan, about 24 h after application of 6.7 GBq ^{177}Lu-PSMA-617. Figure adapted from Eppard et al. Theranostics 2017;7:4359–69.[26] mCRPC, metastasized castration-resistant prostate cancer; MIP, maximum intensity projection; PET, positron emission tomography; PSMA, prostate-specific membrane antigen.

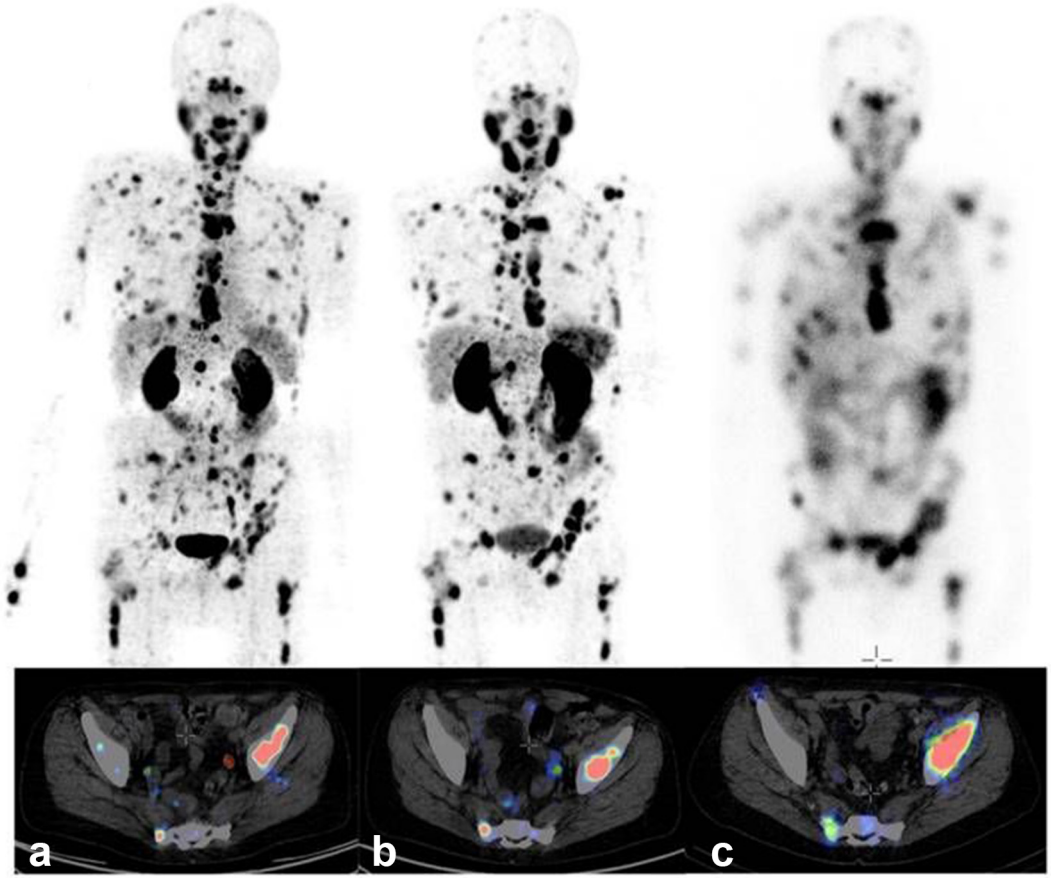

CONCLUSION

Based on the results of (pre)clinical studies, it is clear that ^{44}Sc holds great promise for future applications as a novel PET nuclide for diagnostic imaging and for monitoring therapy in clinics. Whether ^{43}Sc will replace ^{44}Sc in future is unclear and critically dependent on the possibilities of producing it in large quantities and at reasonable cost. The investigation of ^{47}Sc for therapy is still in its infancy and a potential utility for this novel β^--particle-emitting radionuclide has to be defined.

Figure 8. Comparison of serial images of the transverse section of liver, representing the lesion in segment VII (green arrow), obtained by PET/CT imaging of Patient 1 using somatostatin analogs for restaging after the third cycle of PRRT. (a) At 18 months after PRRT, the lesion was not detected on PET/CT image obtained with ^{68}Ga-DOTATOC; (b) at 27 months after PRRT, the lesion was detected using ^{44}Sc-DOTATOC; (c) a concurrent MRI performed within 24 h of the PET/CT scan obtained with ^{44}Sc-DOTATOC co-registered the lesion seen on the PET/CT image; (d) at 36 months after PRRT, the lesion was detected on PET/CT images obtained with ^{68}Ga-DOTATOC. Figure adapted from Singh et al.[31] Cancer Biother Radiopharm 2017;32:124–32 [31] PET, positron emission tomography; PRRT, peptide receptor radionuclide therapy.

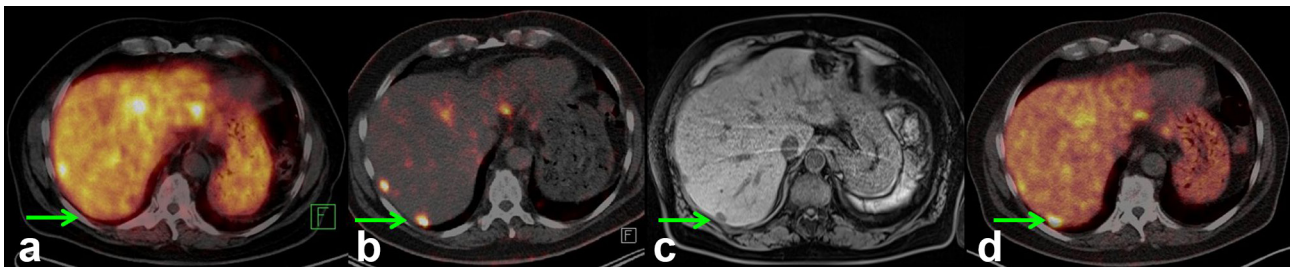

Figure 9. PET/CT images of a patient with neuroendocrine neoplasm of the terminal ileum obtained at 2 h after injection of ^{152}Tb-DOTATOC. (a) MIP image shows the Ki, the UB, the Sp and the IS. (b/c) Transverse sections of PET/CT fusion images demonstrate radiopeptide uptake in lymph node metastases in the right costophrenic region and in the right internal mammary chain (green arrows), as well as in Segment 7 of the liver (blue arrows) and in a skeletal metastasis in the left third rib adjacent to the sternocostal junction (red arrows). Figure adapted from Baum et al. Dalton Trans 2017;46:14638–46.[71] IS, injection site; Ki, kidneys; MIP, maximum intensity projection; Sp, spleen; UB, urinary bladder.

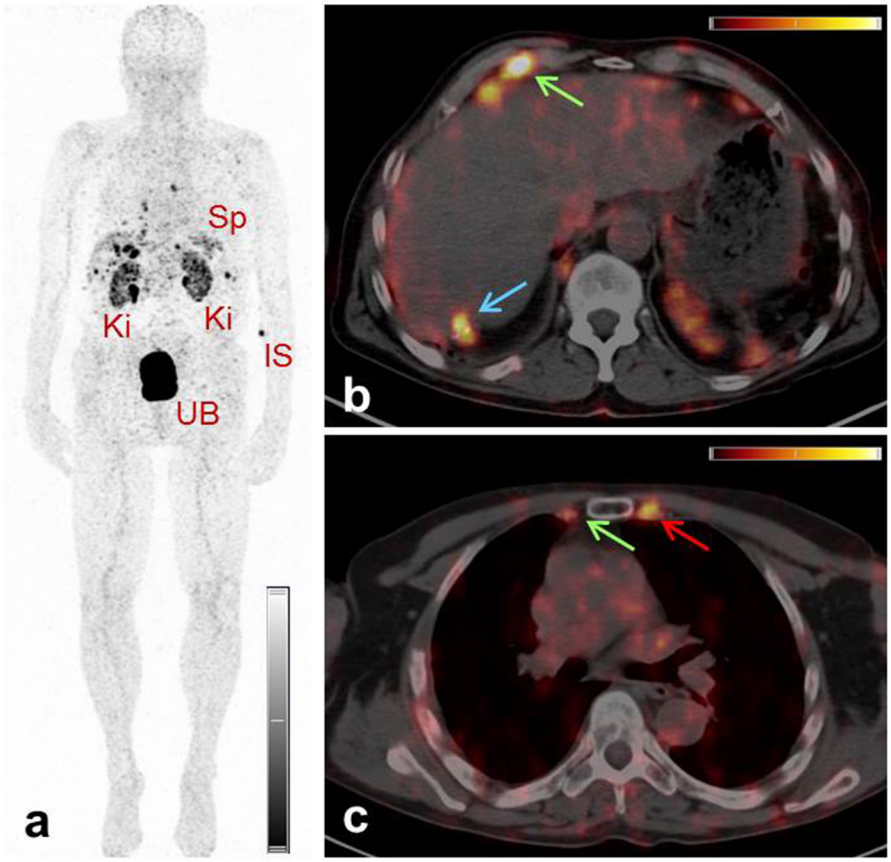

Among the Tb radionuclides, ^{161}Tb is undoubtedly the most advanced in terms of production and pre-clinical investigation. The similarity of ^{161}Tb to ^{177}Lu makes this novel radiolanthanide highly attractive for therapeutic application, potentially enabling a more effective therapy due to the coemission of Auger electrons while using the same targeting agents. ^{155}Tb could be produced at a cyclotron with potentially high yields; significant research efforts in this regard will be necessary, however. As a diagnostic match, ^{155}Tb may be of particular value for visualization and staging of malignancies and for dosimetry calculation prior to therapy with clinically employed and new radiolanthanides, such as ^{177}Lu and ^{161}Tb, respectively.

^{152}Tb and, in particular, the α-particle emitting ^{149}Tb are of interest for clinical application, however, the production of these Tb radioisotopes remains challenging and will only be possible at specific production sites where a mass separator is available. Even though such facilities are currently under construction at several sites worldwide, the general availability of these nuclides may remain scarce, in particular, the short-lived ^{149}Tb which can only be used in close proximity to the production site.

The question on whether it would be beneficial or even essential, to use chemically identical radioligands for diagnosis and therapy is a controversial topic in the community and can only be addressed once the concept of "matched pair" radionuclides is realized in a clinical setting. Taking all relevant aspects into consideration, scandium provides the most promising diagnostic match whereas, in the case of terbium, the therapeutic radioisotopes are of most clinical interest. It is, therefore, possible and likely that $^{43/44}$Sc could be used in tandem with $^{149/161}$Tb, since both elements can be stably coordinated with a DOTA chelator. This means that using the same tumor targeting agent for Sc/Tb-based radiotheranostics would be feasible.

Both scandium and terbium remain of utmost interest for further development, with regard to routine production in large quantities for future application in nuclear medicine. Basic research and more detailed (pre)clinical investigations will be required, to enable the specific aims of individual dose plans for personalized radionuclide therapy and the option of therapy monitoring, as well as therapy regimes tailored to their specific medical situation.

REFERENCES

1. Yordanova A, Eppard E, Kürpig S, Bundschuh RA, Schönberger S, Gonzalez-Carmona M, et al. Theranostics in nuclear medicine practice. *Onco Targets Ther* 2017; **10**: 4821–8. doi: https://doi.org/10.2147/OTT.S140671
2. Ahn BC. Personalized medicine based on theranostic radioiodine molecular imaging for differentiated thyroid cancer. *Biomed Res Int* 2016; **2016**: 1–9. doi: https://doi.org/10.1155/2016/1680464
3. Hertz S, Roberts A. Radioactive iodine as an indicator in thyroid physiology V. The use of radioactive iodine in the differential diagnosis of two types of Graves' disease. *J Clin Invest* 1942; **21**: 31–2. doi: https://doi.org/10.1172/JCI101276
4. Hertz B, Schuller K, Saul Hertz M. Saul Hertz, MD (1905–1950): A pioneer in the use of radioactive Iodine. *Endocr Pract* 2010; **16**: 713–5. doi: https://doi.org/10.4158/EP10065.CO
5. Padma S, Sundaram PS. Radioiodine as an adjuvant therapy and its role in follow-up of differentiated thyroid cancer. *J Cancer Res Ther* 2016; **12**: 1109–13. doi: https://doi.org/10.4103/0973-1482.163677
6. Deppen SA, Blume J, Bobbey AJ, Shah C, Graham MM, Lee P, et al. 68Ga-DOTATATE compared with ^{111}In-DTPA-octreotide and conventional imaging for pulmonary and gastroenteropancreatic neuroendocrine tumors: a systematic review and meta-analysis. *J Nucl Med* 2016; **57**: 872–8. doi: https://doi.org/10.2967/jnumed.115.165803
7. van Vliet EI, Teunissen JJ, Kam BL, de Jong M, Krenning EP, Kwekkeboom DJ. Treatment of gastroenteropancreatic neuroendocrine tumors with peptide receptor radionuclide therapy. *Neuroendocrinology* 2013; **97**: 74–85. doi: https://doi.org/10.1159/000335018
8. Calais J, Fendler WP, Eiber M, Gartmann J, Chu FI, Nickols NG. Actual impact of ^{68}Ga-PSMA-11 PET/CT on the management of prostate cancer patients with biochemical recurrence. *J Nucl Med* 2017.
9. Kulkarni HR, Singh A, Schuchardt C, Niepsch K, Sayeg M, Leshch Y, et al. PSMA-based radioligand therapy for metastatic castration-resistant prostate cancer: the bad berka experience since 2013. *J Nucl Med* 2016; **57**(Suppl 3): 97S–104. doi: https://doi.org/10.2967/jnumed.115.170167
10. Fendler WP, Rahbar K, Herrmann K, Kratochwil C, Eiber M. ^{177}Lu-PSMA radioligand therapy for prostate cancer. *J Nucl Med* 2017; **58**: 1196–200. doi: https://doi.org/10.2967/jnumed.117.191023
11. Kratochwil C, Bruchertseifer F, Giesel FL, Weis M, Verburg FA, Mottaghy F, et al. 225Ac-PSMA-617 for PSMA-targeted α-radiation therapy of metastatic castration-resistant prostate cancer. *J Nucl Med* 2016; **57**: 1941–4. doi: https://doi.org/10.2967/jnumed.116.178673
12. Sathekge M, Knoesen O, Meckel M, Modiselle M, Vorster M, Marx S. ^{213}Bi-PSMA-617 targeted alpha-radionuclide therapy in metastatic castration-resistant prostate cancer. *Eur J Nucl Med Mol Imaging* 2017; **44**: 1099–100. doi: https://doi.org/10.1007/s00259-017-3657-9
13. Müller C, Bunka M, Haller S, Köster U, Groehn V, Bernhardt P, et al. Promising prospects for ^{44}Sc-/^{47}Sc-based theragnostics: application of ^{47}Sc for radionuclide tumor therapy in mice. *J Nucl Med* 2014; **55**: 1658–64. doi: https://doi.org/10.2967/jnumed.114.141614
14. van der Meulen NP, Bunka M, Domnanich KA, Müller C, Haller S, Vermeulen C, et al. Cyclotron production of ^{44}Sc: from bench to bedside. *Nucl Med Biol* 2015; **42**: 745–51. doi: https://doi.org/10.1016/j.nucmedbio.2015.05.005
15. Domnanich KA, Eichler R, Müller C, Jordi S, Yakusheva V, Braccini S, et al. Production and separation of ^{43}Sc for radiopharmaceutical purposes. *EJNMMI Radiopharm Chem* 2017; **2**: 14. doi: https://doi.org/10.1186/s41181-017-0033-9
16. Majkowska-Pilip A, Bilewicz A. Macrocyclic complexes of scandium radionuclides as precursors for diagnostic and therapeutic radiopharmaceuticals. *J Inorg Biochem* 2011; **105**: 313–20. doi: https://doi.org/10.1016/j.jinorgbio.2010.11.003
17. Müller C, Zhernosekov K, Köster U, Johnston K, Dorrer H, Hohn A, et al. A unique matched quadruplet of terbium radioisotopes for PET and SPECT and for α- and β- radionuclide therapy: an in vivo proof-of-concept study with a new receptor-targeted folate derivative. *J Nucl Med* 2012; **53**: 1951–9. doi: https://doi.org/10.2967/jnumed.112.107540
18. Bernhardt P, Benjegård SA, Kölby L, Johanson V, Nilsson O, Ahlman H, et al. Dosimetric comparison of radionuclides for therapy of somatostatin receptor-expressing tumors. *Int J Radiat Oncol Biol Phys* 2001; **51**: 514–24. doi: https://doi.org/10.1016/S0360-3016(01)01663-7
19. Lehenberger S, Barkhausen C, Cohrs S, Fischer E, Grünberg J, Hohn A, et al. The low-energy β$^-$ and electron emitter ^{161}Tb as an alternative to ^{177}Lu for targeted radionuclide therapy. *Nucl Med Biol* 2011; **38**: 917–24. doi: https://doi.org/10.1016/j.nucmedbio.2011.02.007
20. Champion C, Quinto MA, Morgat C, Zanotti-Fregonara P, Hindié E. Comparison between three promising β-emitting radionuclides, ^{67}Cu, ^{47}Sc and ^{161}Tb, with emphasis on doses delivered to minimal residual disease. *Theranostics* 2016; **6**: 1611–8. doi: https://doi.org/10.7150/thno.15132
21. Beyer GJ, Čomor JJ, Daković M, Soloviev D, Tamburella C, Hagebø E, et al. Production routes of the alpha emitting ^{149}Tb for medical application. *Radiochim Acta* 2002; **90**: 247–52. doi: https://doi.org/10.1524/ract.2002.90.5_2002.247
22. Rösch F, Baum RP. Generator-based PET radiopharmaceuticals for molecular imaging of tumours: on the way to THERANOSTICS. *Dalton Trans* 2011; **40**: 6104–11. doi: https://doi.org/10.1039/c0dt01504k
23. Filosofov DV, Loktionova NS, Rösch F. A ^{44}Ti/^{44}Sc radionuclide generator for potential application of ^{44}Sc-based PET-radiopharmaceuticals. *Radiochim Acta* 2010; **98**: 149. doi: https://doi.org/10.1524/ract.2010.1701
24. Pruszyński M, Loktionova NS, Filosofov DV, Rösch F. Post-elution processing of ^{44}Ti/^{44}Sc generator-derived ^{44}Sc for clinical application. *Appl Radiat Isot* 2010; **68**: 1636–41. doi: https://doi.org/10.1016/j.apradiso.2010.04.003
25. Roesch F. Scandium-44: benefits of a long-lived PET radionuclide available from the 44Ti/44Sc generator system. *Curr Radiopharm* 2012; **5**: 187–201. doi: https://doi.org/10.2174/1874471011205030187
26. Eppard E, de la Fuente A, Benešová M, Khawar A, Bundschuh RA, Gärtner FC, et al. Clinical translation and first in-human use of [^{44}Sc]Sc-PSMA-617 for PET imaging of metastasized castrate-resistant prostate cancer. *Theranostics* 2017; **7**: 4359–69. doi: https://doi.org/10.7150/thno.20586
27. Severin GW, Engle JW, Valdovinos HF, Barnhart TE, Nickles RJ. Cyclotron produced ^{44g}Sc from natural calcium. *Appl Radiat Isot* 2012; **70**: 1526–30. doi: https://doi.org/10.1016/j.apradiso.2012.04.030
28. Valdovinos HF, Hernandez R, Barnhart TE, Graves S, Cai W, Nickles RJ. Separation of cyclotron-produced ^{44} Sc from a natural calcium target using a dipentyl pentylphosphonate functionalized extraction resin. *Applied Radiation and Isotopes* 2015; **95**: 23–9. doi: https://doi.org/10.1016/j.apradiso.2014.09.020

29. Krajewski S, Cydzik I, Abbas K, Bulgheroni A, Simonelli F, Holzwarth U, et al. Cyclotron production of ^{44}Sc for clinical application. *Radiochim Acta* 2013; **101**: 333–8. doi: https://doi.org/10.1524/ract.2013.2032
30. Müller C, Bunka M, Reber J, Fischer C, Zhernosekov K, Türler A, et al. Promises of cyclotron-produced 44Sc as a diagnostic match for trivalent β-emitters: in vitro and in vivo study of a 44Sc-DOTA-folate conjugate. *J Nucl Med* 2013; **54**: 2168–74. doi: https://doi.org/10.2967/jnumed.113.123810
31. Singh A, van der Meulen NP, Müller C, Klette I, Kulkarni HR, Türler A, et al. First-in-human PET/CT imaging of metastatic neuroendocrine neoplasms with cyclotron-produced ^{44}Sc-DOTATOC: a proof-of-concept study. *Cancer Biother Radiopharm* 2017; **32**: 124–32. doi: https://doi.org/10.1089/cbr.2016.2173
32. Walczak R, Krajewski S, Szkliniarz K, Sitarz M, Abbas K, Choiński J, et al. Cyclotron production of ^{43}Sc for PET imaging. *EJNMMI Phys* 2015; **2**: 33. doi: https://doi.org/10.1186/s40658-015-0136-x
33. Szkliniarz K, Jastrzębski J, Bilewicz A, Chajduk E, Choiński J, Jakubowski A, et al. Medical radioisotopes produced using the alpha particle beam from the Warsaw heavy Ion cyclotron. *Acta Physica Polonica A* 2015; **127**: 1471–4. doi: https://doi.org/10.12693/APhysPolA.127.1471
34. Szkliniarz K, Sitarz M, Walczak R, Jastrzębski J, Bilewicz A, Choiński J, et al. Production of medical Sc radioisotopes with an alpha particle beam. *Appl Radiat Isot* 2016; **118**: 182–9. doi: https://doi.org/10.1016/j.apradiso.2016.07.001
35. Minegishi K, Nagatsu K, Fukada M, Suzuki H, Ohya T, Zhang MR. Production of scandium-43 and -47 from a powdery calcium oxide target via the $^{nat/44}$Ca(α,x)-channel. *Appl Radiat Isot* 2016; **116**: 8–12. doi: https://doi.org/10.1016/j.apradiso.2016.07.017
36. Bunka M, Müller C, Vermeulen C, Haller S, Türler A, Schibli R, et al. Imaging quality of ^{44}Sc in comparison with five other PET radionuclides using Derenzo phantoms and preclinical PET. *Appl Radiat Isot* 2016; **110**: 129–33. doi: https://doi.org/10.1016/j.apradiso.2016.01.006
37. Misiak R, Walczak R, Wąs B, Bartyzel M, Mietelski JW, Bilewicz A. 47Sc production development by cyclotron irradiation of Ca. *J Radioanal Nucl Chem* 2017; **313**: 429–34. doi: https://doi.org/10.1007/s10967-017-5321-z
38. Domnanich KA, Müller C, Benešová M, Dressler R, Haller S, Köster U, et al. ^{47}Sc as useful β$^-$emitter for the radiotheragnostic paradigm: a comparative study of feasible production routes. *EJNMMI Radiopharm Chem* 2017; **2**: 5. doi: https://doi.org/10.1186/s41181-017-0024-x
39. Kolsky KL, Joshi V, Mausner LF, Srivastava SC. Radiochemical purification of no-carrier-added scandium-47 for radioimmunotherapy. *Appl Radiat Isot* 1998; **49**: 1541–9. doi: https://doi.org/10.1016/S0969-8043(98)00016-5
40. Bartoś B, Majkowska A, Krajewski S, Bilewicz A. New separation method of no-carrier-added ^{47} Sc from titanium targets. *Radiochim Acta* 2012; **100**: 457–62. doi: https://doi.org/10.1524/ract.2012.1938
41. Rane S, Harris JT, Starovoitova VN. 47Ca production for ^{47}Ca/^{47}Sc generator system using electron linacs. *Appl Radiat Isot* 2015; **97**: 188–92. doi: https://doi.org/10.1016/j.apradiso.2014.12.020
42. Mamtimin M, Harmon F, Starovoitova VN. Sc-47 production from titanium targets using electron linacs. *Appl Radiat Isot* 2015; **102**: 1–4. doi: https://doi.org/10.1016/j.apradiso.2015.04.012
43. Yagi M, Kondo K. Preparation of carrier-free ^{47}Sc by the ^{48}Ti(γ,p) reaction. *Int J Appl Radiat Isot* 1977; **28**: 463–8. doi: https://doi.org/10.1016/0020-708X(77)90178-8
44. Rotsch DA, Brown MA, Nolen JA, Brossard T, Henning WF, Chemerisov SD, et al. Electron linear accelerator production and purification of scandium-47 from titanium dioxide targets. *Appl Radiat Isot* 2018; **131**: 77–82. doi: https://doi.org/10.1016/j.apradiso.2017.11.007
45. Starovoitova VN, Cole PL, Grimm TL. Accelerator-based photoproduction of promising β-emitters 67Cu and 47Sc. *J Radioanal Nucl Chem* 2015; **305**: 127–32. doi: https://doi.org/10.1007/s10967-015-4039-z
46. Vermeulen C, Steyn GF, Szelecsényi F, Kovács Z, Suzuki K, Nagatsu K, et al. Cross sections of proton-induced reactions on ^{nat}Gd with special emphasis on the production possibilities of ^{152}Tb and ^{155}Tb. *Nucl Instrum Methods Phys Res Sect B-Beam Interact Mater Atoms* 2012; **275**: 24–32. doi: https://doi.org/10.1016/j.nimb.2011.12.064
47. Allen BJ, Goozee G, Sarkar S, Beyer G, Morel C, Byrne AP. Production of terbium-152 by heavy ion reactions and proton induced spallation. *Appl Radiat Isot* 2001; **54**: 53–8. doi: https://doi.org/10.1016/S0969-8043(00)00164-0
48. Köster U, Collaboration I. ISOLDE target and ion source chemistry. *Radiochim Acta* 2001; **89**:749–56. doi: https://doi.org/10.1524/ract.2001.89.11-12.749
49. Połosak M, Piotrowska A, Krajewski S, Bilewicz A. Stability of ^{47}Sc-complexes with acyclic polyamino-polycarboxylate ligands. *J Radioanal Nucl Chem* 2013; **295**: 1867–72. doi: https://doi.org/10.1007/s10967-012-2188-x
50. Kerdjoudj R, Pniok M, Alliot C, Kubíček V, Havlíčková J, Rösch F, et al. Scandium(III) complexes of monophosphorus acid DOTA analogues: a thermodynamic and radiolabelling study with ^{44}Sc from cyclotron and from a ^{44}Ti/^{44}Sc generator. *Dalton Trans* 2016; **45**: 1398–409. doi: https://doi.org/10.1039/c5dt04084a
51. Nagy G, Szikra D, Trencsényi G, Fekete A, Garai I, Giani AM, et al. AAZTA: An ideal chelating agent for the development of ^{44}Sc PET imaging agents. *Angew Chem Int Ed Engl* 2017; **56**: 2118–22. doi: https://doi.org/10.1002/anie.201611207
52. Chakravarty R, Goel S, Valdovinos HF, Hernandez R, Hong H, Nickles RJ, et al. Matching the decay half-life with the biological half-life: ImmunoPET imaging with ^{44}Sc-labeled cetuximab Fab fragment. *Bioconjug Chem* 2014; **25**: 2197–204. doi: https://doi.org/10.1021/bc500415x
53. Koumarianou E, Pawlak D, Korsak A, Mikolajczak R. Comparison of receptor affinity of ^{nat}Sc-DOTA-TATE versus ^{nat}Ga-DOTA-TATE. *Nucl Med Rev Cent East Eur* 2011; **14**: 85–9. doi: https://doi.org/10.5603/NMR.2011.00021
54. Pruszyński M, Majkowska-Pilip A, Loktionova NS, Eppard E, Roesch F. Radiolabeling of DOTATOC with the long-lived positron emitter ^{44}Sc. *Appl Radiat Isot* 2012; **70**: 974–9. doi: https://doi.org/10.1016/j.apradiso.2012.03.005
55. Domnanich KA, Müller C, Farkas R, Schmid RM, Ponsard B, Schibli R, et al. 44Sc for labeling of DOTA- and NODAGA-functionalized peptides: preclinical in vitro and in vivo investigations. *EJNMMI Radiopharm Chem* 2017; **1**: 8. doi: https://doi.org/10.1186/s41181-016-0013-5
56. Koumarianou E, Loktionova NS, Fellner M, Roesch F, Thews O, Pawlak D, et al. 44Sc-DOTA-BN[$_2$-14]NH$_2$ in comparison to ^{68}Ga-DOTA-BN[$_2$-14]NH$_2$ in pre-clinical investigation. *Is 44Sc a potential radionuclide for PET? Appl Radiat Isot* 2012; **70**: 2669–76.
57. Hernandez R, Valdovinos HF, Yang Y, Chakravarty R, Hong H, Barnhart TE, et al. ^{44}Sc: an attractive isotope for peptide-based PET imaging. *Mol Pharm* 2014; **11**: 2954–61. doi: https://doi.org/10.1021/mp500343j
58. Umbricht CA, Benešová M, Schmid RM, Türler A, Schibli R, van der Meulen NP, et al. ^{44}Sc-PSMA-617 for radiotheragnostics in tandem with ^{177}Lu-PSMA-617-preclinical investigations in comparison with ^{68}Ga-

PSMA-11 and ^{68}Ga-PSMA-617. *EJNMMI Res* 2017; **7**: 9. doi: https://doi.org/10.1186/s13550-017-0257-4

59. Eigner S, Vera DR, Fellner M, Loktionova NS, Piel M, Lebeda O, et al. Imaging of protein synthesis: in vitro and in vivo evaluation of ^{44}Sc-DOTA-puromycin. *Mol Imaging Biol* 2013; **15**: 79–86. doi: https://doi.org/10.1007/s11307-012-0561-3
60. Honarvar H, Müller C, Cohrs S, Haller S, Westerlund K, Karlström AE, et al. Evaluation of the first ^{44}Sc-labeled Affibody molecule for imaging of HER2-expressing tumors. *Nucl Med Biol* 2017; **45**: 15–21. doi: https://doi.org/10.1016/j.nucmedbio.2016.10.004
61. Löfblom J, Feldwisch J, Tolmachev V, Carlsson J, Ståhl S, Frejd FY. Affibody molecules: engineered proteins for therapeutic, diagnostic and biotechnological applications. *FEBS Lett* 2010; **584**: 2670–80. doi: https://doi.org/10.1016/j.febslet.2010.04.014
62. Müller C, Vermeulen C, Johnston K, Köster U, Schmid R, Türler A, et al. Preclinical in vivo application of ^{152}Tb-DOTANOC: a radiolanthanide for PET imaging. *EJNMMI Res* 2016; **6**: 35. doi: https://doi.org/10.1186/s13550-016-0189-4
63. Müller C, Fischer E, Behe M, Köster U, Dorrer H, Reber J, et al. Future prospects for SPECT imaging using the radiolanthanide terbium-155 - production and preclinical evaluation in tumor-bearing mice. *Nucl Med Biol* 2014; **41**: e58–e65. doi: https://doi.org/10.1016/j.nucmedbio.2013.11.002
64. Beyer GJ, Miederer M, Vranjes-Durić S, Comor JJ, Künzi G, Hartley O, et al. Targeted alpha therapy in vivo: direct evidence for single cancer cell kill using ^{149}Tb-rituximab. *Eur J Nucl Med Mol Imaging* 2004; **31**: 547–54. doi: https://doi.org/10.1007/s00259-003-1413-9
65. Müller C, Reber J, Haller S, Dorrer H, Köster U, Johnston K, et al. Folate receptor targeted alpha-therapy using terbium-149. *Pharmaceuticals* 2014; **7**: 353–65. doi: https://doi.org/10.3390/ph7030353
66. Müller C, Vermeulen C, Köster U, Johnston K, Türler A, Schibli R, et al. Alpha-PET with terbium-149: evidence and perspectives for radiotheragnostics. *EJNMMI Radiopharm Chem* 2017; **1**: 5. doi: https://doi.org/10.1186/s41181-016-0008-2
67. de Jong M, Breeman WA, Bernard BF, Rolleman EJ, Hofland LJ, Visser TJ, et al. Evaluation in vitro and in rats of ^{161}Tb-DTPA-octreotide, a somatostatin analogue with potential for intraoperative scanning and radiotherapy. *Eur J Nucl Med* 1995; **22**: 608–16. doi: https://doi.org/10.1007/BF01254561
68. Müller C, Reber J, Haller S, Dorrer H, Bernhardt P, Zhernosekov K, et al. Direct in vitro and in vivo comparison of ^{161}Tb and $^{(177}$Lu using a tumour-targeting folate conjugate. *Eur J Nucl Med Mol Imaging* 2014; **41**: 476–85. doi: https://doi.org/10.1007/s00259-013-2563-z
69. Haller S, Pellegrini G, Vermeulen C, van der Meulen NP, Köster U, Bernhardt P, et al. Contribution of Auger/conversion electrons to renal side effects after radionuclide therapy: preclinical comparison of ^{161}Tb-folate and ^{177}Lu-folate. *EJNMMI Res* 2016; **6**: 13. doi: https://doi.org/10.1186/s13550-016-0171-1
70. Grünberg J, Lindenblatt D, Dorrer H, Cohrs S, Zhernosekov K, Köster U, et al. Anti-L1CAM radioimmunotherapy is more effective with the radiolanthanide terbium-161 compared to lutetium-177 in an ovarian cancer model. *Eur J Nucl Med Mol Imaging* 2014; **41**: 1907–15. doi: https://doi.org/10.1007/s00259-014-2798-3
71. Baum RP, Singh A, Benešová M, Vermeulen C, Gnesin S, Köster U, et al. Clinical evaluation of the radiolanthanide terbium-^{152}: first-in-human PET/CT with ^{152}Tb-DOTATOC. *Dalton Trans* 2017; **46**: 14638–46. doi: https://doi.org/10.1039/C7DT01936J